Available online at www.sciencedirect.com

ScienceDirect

Mendeleev Commun., 2020, **30**, 84–87

Mendeleev Communications

Intrinsic infrared absorption for carbon–fluorine bonding in fluorinated nanodiamond

Vladimir Yu. Osipov,*[a,b] Nikolai M. Romanov,[c,d] Kenta Kogane,[b] Hidekazu Touhara,[e] Yoshiyuki Hattori[e] and Kazuyuki Takai[b]

[a] *Ioffe Institute, Russian Academy of Sciences, 194021 St. Petersburg, Russian Federation. E-mail: osipov@mail.ioffe.ru*
[b] *Department of Chemical Science and Technology, Hosei University, 184-8584 Tokyo, Japan*
[c] *School of Engineering Science, LUT University, 53850 Lappeenranta, Finland*
[d] *Peter the Great St. Petersburg Polytechnic University, 195251 St. Petersburg, Russian Federation*
[e] *Department of Textile Science and Technology, Shinshu University, 386-8567 Ueda, Nagano, Japan*

DOI: 10.1016/j.mencom.2020.01.028

IR spectroscopy of fluorinated detonation nanodiamond demonstrates that an intense absorption band at ~1344 cm^{-1} and two smaller ones at ~1324 and ~1258 cm^{-1} form the extended low wave-number wing of the observed consolidated spectrum in the range of 1100–1400 cm^{-1}. The intrinsic infrared absorption of CF_x bonding at the nanodiamond surface sites has been determined after subtraction of the contribution from remaining C–O and C–O–C groups inside the aggregates of tightly-bonded fundamental nanodiamond particles, which had not been subjected to fluorine attack and to their replacement by fluorine containing groups.

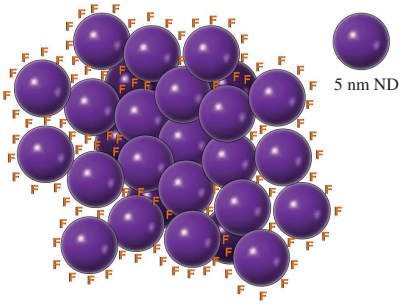

Keywords: detonation nanodiamond, surface chemistry, fluorination, carbon–fluorine bonding, infrared spectroscopy.

Detonation nanodiamonds (DND) with mean size of about 5 nm are very promising objects for investigation because of their potential use for enforcement and the life cycle extension of various soft materials including resins and plastics.[1] DND and their various surface modified derivatives have been analyzed in terms of both surface chemistry as well as origin of target alien molecules and ligands.[2–5] The surface of ordinary as-fabricated DND particles is hydrophilic and predominantly covered with various oxygen-containing functional groups, mainly carboxyl and hydroxyl, which give a way to bind additional alien molecular agents and metal cations from an environment.[6] Nevertheless, in some specific applications a hydrophobic surface is favorable. In this case, complete coverage of DND surface by fluorine atoms is one of the potential strategies to achieve the hydrophobicity. Earlier[7,8] we clarified the identifying features of the functional groups on the DND surface using IR spectroscopy. Although the first results on IR absorption of fluorinated DND were reported about 15 years ago,[9–12] up to now no serious attention has been paid to the comprehensive analysis of parameters of a number of IR absorption bands related to CF_x sites on the surface of fluorinated nanodiamonds, especially in the case of large fluorine (up to 18 at%) and small oxygen (down to 1.5 at%) content. Only several works on IR absorption/reflectance spectroscopy of directly fluorinated diamond surface have been carried out.[13,14] The diamond particles of DND differ from those in other nanodiamonds, which have a diameter larger than 10 nm and are obtained by milling the natural type IIa microdiamonds with low nitrogen content (< 10 ppm) or from Ib microdiamonds synthesized at high pressure and high temperature with nitrogen content less than 300 ppm. In the case of DND, nitrogen impurities usually constitute up to ~2.5 at% and are distributed mainly homogeneously in the covalent lattice of the diamond core, although the enrichment of nitrogen near the grain boundaries or twinning boundaries has been noted.[15,16] The embedded nitrogen is predominantly present in the diamond lattice in the form of magnetically silent NN dimers.[15,16] It hints that DND belongs to the type Ia of diamond. This elevated concentration of nitrogen impurities in DND can be responsible for its remarkable reactivity towards aggressive etching agents. Moreover, the fundamental nanodiamond particles with a diameter of 5 nm are aggregated in DND, where each particle is typically tightly bound by organic anhydride groups containing C–O and C–O–C bondings.

In this work, we used commercially available extra purified DND and functionalized their surface with oxygen-containing groups. Weakly bound adsorbates and alien molecular agents were removed from the surface of sample ND-1 by heating in air at 350 °C. In general, oxygen-containing groups can be introduced into the surface of sample ND-1 due to oxidative conditions of this process, although it does not practically change the composition of the surface functional groups containing C–O and C–O–C bonds. The accomplishment of this procedure was confirmed in our earlier works.[17,18] The surface of DND particles was thereafter chemically modified using direct fluorination *via* exposure to fluorine gas as described.[†,18,19] Hereafter, the DND samples treated by fluorine

[†] For fluorination, a nickel reactor and equipment of Shinshu University (Japan) and fluorine gas (purity 99.7%) produced by Daikin Industries, Ltd. (Japan) were used. No essential loss of mass was detected for DND

gas at 350 and 500 °C for 3 days were labelled as ND-2 and ND-3. It was shown by X-ray photoelectron spectroscopy (XPS)‡ that the content of nitrogen and the surface oxygen in sample ND-1 as the starting material was 2.0 and 8.2 at%, respectively. The latter comes from the oxygen-containing groups on surface of the nanodiamond particle. The fluorine content for the nanodiamonds fluorinated at 350 (ND-2) and 500 °C (ND-3) was estimated as 15 and 18 at%, respectively, while the oxygen content drops from 3.6 to 1.3 at% after elevation of fluorination temperature from 350 to 500 °C. The concentration of interior nitrogen did not change during the fluorination and was about 1.9 at%. For samples ND-2 and ND-3, the atomic ratio F/C was ~0.21 ± 0.15. Such atomic composition is valuable in terms of the number of fluorine atoms sited on the surface of DND particles. A model DND as a 5 nm spherical particle consisting of ~11500 carbon atoms has only ~1300 (or ~11%) carbon atoms located on the surface, which can be terminated by alien agents *via* σ-bonds. It means that almost all of the DND surface was fluorinated in the sp^3 CF and sp^3 CF_2 manner, although some oxygen-containing functional groups were present inside the aggregates of the nanodiamond particles tightly bound by anhydride groups in DND. The excess of F/C ratio above 11% could be attributed to the penetration of some fluorine atoms inside the diamond surface lattice and their attack on the sp^3 C–C bonds§ along with the slightly smaller actual size of the diamond crystallites, namely ~4.3 nm.

The IR absorption spectra of samples ND-1, ND-2 and ND-3 in the range of 800–2200 cm^{-1} are shown in Figure 1.¶ All initial transmission spectra were converted into the absorption spectra and normalized in order to have the same absorption values and the same shapes of the low frequency wings in the range of 800–1100 cm^{-1}, since the absorption in this range is associated with C–O and C–O–C groups as, *e.g.,* for as-fabricated acid treated pristine DND sample ND-1 with a surface functionalized only by oxygen-containing groups. An additional clue for the normalization of spectra for the reliable comparison of contributions from various chemical functional groups results from consideration of the intensities of ~1632 cm^{-1} peaks, which are attributed to hydroxyl groups at the DND surface or to adsorbed water in KBr pellet. The intensities of these peaks are normalized to be fairly close for both spectra in Figure 1(*b*). The alignment is almost the same for low frequency wing at 800–1100 cm^{-1} and for the valley between the absorption bands at ~1340 and ~1632 cm^{-1} for the normalized spectra of samples ND-2 and ND-3. The main difference in IR spectra for fluorinated and non-fluorinated samples comes in the range above 1130 cm^{-1}. Thus, the spectrum of ND-1 demonstrates several superimposed neighbouring bands associated with C–O–C and C–O (800–1450 cm^{-1}), O–H (~1628 cm^{-1}) and C=O (~1742 cm^{-1}) absorptions. Bands located between 800 and 1500 cm^{-1} form a rough triangle with maximum at ~1130 cm^{-1} and smoothly falling area in the range of 1130–1500 cm^{-1} [Figure 1(*a*)]. Absorption band at ~1628 cm^{-1} is usually assigned to water

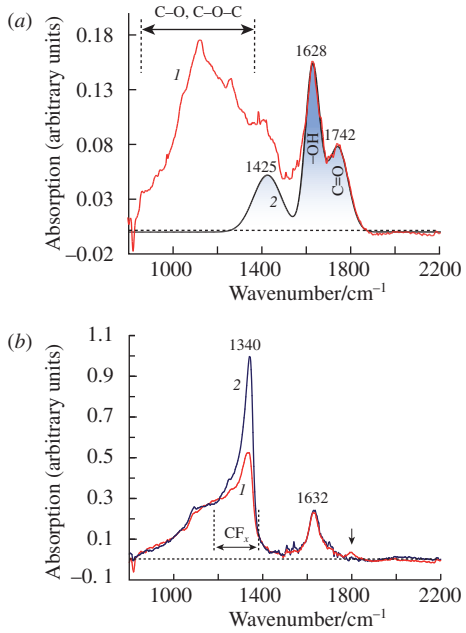

Figure 1 IR absorption spectra of (*a*) pristine acid-purified DND: (*1*) sample ND-1, (*2*) sum of the three Gaussian shape bands associated with carbonyl (~1742 cm^{-1}) and hydroxyl (~1628 cm^{-1}) groups as well as some other easily replaced surface groups disappeared after fluorination (~1425 cm^{-1}) and (*b*) DNDs fluorinated at: (*1*) 350 °C (sample ND-2), (*2*) 500 °C (sample ND-3) for pellets pressed from 2 : 1000 DND–KBr mixtures, the intensities of ~1632 cm^{-1} bands associated with hydroxyl groups and remaining adsorbed water being made the same for spectra (*1*) and (*2*) in the panel.

adsorbed on the surface of DND particles and their aggregates, *i.e.* the alien agent from ambient air, whereas the absorption band at ~1742 cm^{-1} belongs to C=O bonds of carboxyl groups that terminated the surface of nanoparticles and their aggregates. These exterior groups can be easily removed or replaced by other ones upon treatment including the reduction in molecular hydrogen or heat treatment *in vacuo*, that is why the nanodiamond surface chemistry is rather diverse.[20]

The fluorination removes C=O groups from surface. The IR absorption spectra of samples ND-2 and ND-3 [see Figure 1(*b*)] do not contain distinctive absorption bands above 1500 cm^{-1} except for the medium-intensity absorption band at ~1630 cm^{-1} and a strong one at ~3430 cm^{-1} (not shown), attributed to hydroxyl vibrations of adsorbed water.†† Note that a very faint peak at ~1800 cm^{-1} in Figure 1(*b*) is probably related to carbonyl groups from the remaining anhydride on the surface. Similar band was observed in the spectrum of sample ND-2 but disappeared in the ND-3 one. We found that the same few superimposed absorption bands ranging from 800 to 1450 cm^{-1} as in precursor ND-1 (except for the band centered at ~1425 cm^{-1}) were still present in the spectra of fluorinated DND samples [see Figure 2(*b*) for ND-3]. The probable reason is that the oxygen-containing groups responsible for the observed bands are buried deep inside the DND aggregates, and this hampers the approach of fluorine atoms to these groups,‡‡ resulting in their incomplete substitution by fluorination. We found that, besides the ~1740 cm^{-1} band associated with carbonyl, only the band centered at ~1425 cm^{-1} and consequently the corresponding group were completely removed as a result of fluorination. For this reason,

powders treated in fluorine at temperatures 350–500 °C, namely the loss was no more than 20%.

‡ The XPS study was performed on a Perkin-Elmer PHI 5600 Multi-Technique XPS system of Hosei University (Japan) with monochromatized Al-Kα radiation.

§ Some clue in favor of this hypothesis, namely the breaking C–C bonds and penetration under the surface, comes from observation of the several times increase in the amount of dangling bond spins in samples ND-2 and ND-3 according to the EPR data.

¶ The IR absorption spectra were recorded in Ioffe Institute (Russia) on a Carl Zeiss Jena Specord-M80 IR spectrometer (Germany) using pressed transparent tablets prepared from 2 : 1000 or 4 : 1000 mixture of DND powder and spectroscopic quality KBr (Uvasol®, Merck, Germany). Spectra in both panels (*a*, *b*) of Figure 1 are presented on different vertical scale for easy viewing.

†† Note that water mentioned above remains both in the KBr pellet itself and on the surface of DND particles in the absorbed form after sintering the pellet having a small content of DND powder (~4 : 1000). Water is present even after continuous evacuation of the powder mixture in a press chamber.

‡‡ The model of DND aggregate is shown in the Graphical Abstract. Its central part consists of individual 5 nm particles tightly bonded together by C–O–C groups.

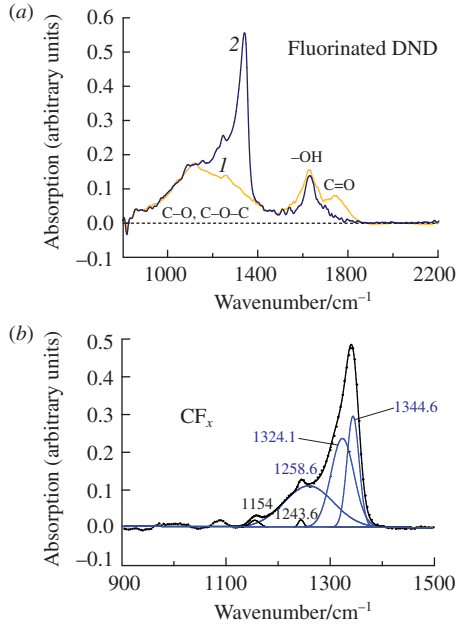

Figure 2 (*a*) IR absorption spectra normalized by intensity of the left wing at ~1070 cm^{-1} and the same superimposed on plot: (*1*) pristine sample ND-1 after subtracting the band at ~1425 cm^{-1}; (*2*) fluorinated sample ND-3 and (*b*) differential IR spectrum obtained after subtraction of the spectrum *1* on panel (*a*) from spectrum *2*.

to determine the intrinsic IR spectrum of fluorine-containing groups on the DND surface, it was necessary to subtract the IR absorption bands of O-containing sites (found, for example, in the reference sample ND-1) from the spectrum of fluorinated samples ND-2 or ND-3. This intrinsic spectrum can be decomposed with three main intensive bands centered at ~1344, ~1324 and ~1258 cm^{-1}. A similar differential spectrum can also be obtained by subtraction of the spectra of fluorinated samples ND-3 and ND-2. The higher the temperature of fluorination treatment, the more pronounced the high-frequency absorption peak at ~1344 cm^{-1}. The differential spectrum of samples ND-3 and ND-2 can be also decomposed with bands centered at ~1344, ~1323 and ~1258 cm^{-1}, similar to Figure 2(*b*). Two of them, namely at ~1344 and ~1258 cm^{-1}, result from stretching vibrations of CF, CF$_2$, CF$_3$ groups. It seems that these bands are the basic features of fluorinated diamond surface because the corresponding absorption lines have been also observed in the form of narrow lines centered at ~1251 and ~1347 cm^{-1} in the absorption spectrum of fluorinated microdiamond with the size less than 0.5 μm and having another morphology.[13]

The band at ~1324 cm^{-1} appears to be an absorption band resulted from Raman scattering of diamond phase through the induced dipole moment of the C–C bonds of the diamond lattice having the neighbouring surface CF bonds in close proximity. This Raman band of 5 nm DND particles is centered at ~1324 cm^{-1} and has the full width at half maximum (FWHM) of ~34 cm^{-1}, whereas for our fluorinated samples the absorption band found in the same location is a little bit wider and has FWHM of ~53 cm^{-1}. The pronounced low-frequency asymmetric wing of the neighbouring poorly distinguishable ~1324 and ~1344 cm^{-1} absorption bands [see Figure 2(*b*)] may also result from Raman scattering activated in the same way for a fraction of nanoparticles with size smaller than 3 nm, while the more probable origin of ~1258 cm^{-1} band is the absorption attributed to CF$_x$ groups. This last band is the widest (FWHM is ~112 cm^{-1} and integrated area is 37%) among the main three absorption bands presented in Figure 2(*b*) and resembles one at ~1240 cm^{-1} for fluorinated amorphous carbon *a*-C:F with increased sp^3 bond ratio as well as fluorinated diamond-like films grown by CVD method.[21,22] Also, PTFE films deposited by sputtering using plasma-assisted method demonstrate the same broad IR absorption band at ~1240 cm^{-1} with an extension from 1100 to 1400 cm^{-1} at the level of ~0.1 of peak maximum. In both known instances, such bands are associated with CF$_x$, mainly CF$_2$ and CF, groups having various local environmental. Bands with peaks centered continuously between ~1120 and ~1340 cm^{-1} are attributed to CF$_3$ and CF$_2$ symmetric stretch, CF$_2$ asymmetric stretch as well as CF=CF$_2$, CF$_3$–CF$_2$ and CF stretch vibrations.[21] However, the main feature of our fluorinated DND in comparison with *a*-C:F films appears from the presence of the two more intensive high frequency absorption bands at > 1300 cm^{-1}. The bands at ~1324 and ~1344 cm^{-1} may be also associated with CF=CF$_2$ (~1324 cm^{-1}) as well as CF$_3$–CF$_2$ and CF stretch (~1344 cm^{-1}) vibrations, but the considerable activation of Raman frequency for C–C vibrations in the nanodiamond lattice seems to represent a more acceptable explanation for the appearance of a strong absorption band at ~1324 cm^{-1}. Note that the δ-like shape and extended low-frequency wing for absorption band of fluorinated micron-sized diamond powder[13,14] are similar to those found for DND, and the two bands centered at 1251–1258 cm^{-1} and 1344–1347 cm^{-1} with uncertainty of position ~5 cm^{-1} are present in the IR spectra in both cases for initially oxidized diamond surface.

Thus, exclusion of the IR absorption bands associated with the remaining C–O, C–O–C and other oxygen- or nitrogen-containing groups in fluorinated DND allowed us to define the absorption bands caused by stretching vibrations of CF$_x$ bonds located on the fluorinated DND surface.

In summary, we have found the main IR absorption bands associated with stretching vibrations of CF$_x$ groups on the surface of fluorinated DND. To define these bands correctly, the sophisticated procedure was applied for the separation of extended superimposed IR absorption bands from the bands of remaining hard-to-remove oxygen-containing groups, which are located inside the DND aggregates or on the part of DND surface not subjected to fluorination. The main absorption bands with integrated intensity of 62% in total occur at ~1324 and ~1344 cm^{-1}, while another less intensive but broader band is centered at ~1258 cm^{-1}. This work opens the way for reliable characterization of fluorocarbon functional groups on the nanodiamond surface. Such fluorinated DND, possessing the outstanding characteristics including high temperature of decomposition and mechanical strength, can serve as fillers in various composites based on fluorocarbon plastics.

V.Yu.O. acknowledges the support from Ioffe Institute (project no. 0040-2014-0013) as well as the Japan Society for the Promotion of Science and JSPS Fellowship (no. L17526). K.T. acknowledges the support from JSPS KAKENHI (grant nos. 16K05758, 19K05410 and 26107532).

References

1 *Detonation Nanodiamonds: Science and Applications*, eds. A. Vul' and O. Shenderova, Pan Stanford Publishing, Singapore, 2014.
2 *Nanodiamonds: Advanced Material Analysis*, *Properties and Applications*, ed. J.-C. Arnault, Elsevier, Amsterdam, 2017.
3 A. Krueger, in *Nanoscience. Book 31. Nanodiamond*, ed. O. A. Williams, Royal Society of Chemistry, Cambridge, 2014, pp. 49–88.
4 M. V. Baidakova, V. Yu. Osipov, C. Katsuyama, K. Takai, T. Enoki, A. Yonemoto, H. Touhara and A. Ya. Vul, in *Multifunctional Conducting Molecular Materials*, eds. G. Saito, F. Wudl, R. C. Haddon, K. Tanigaki, T. Enoki, H. E. Katz and M. Maesato, Special publication No. 306, Royal Society of Chemistry, Cambridge, 2007, pp. 224–231.
5 V. Petrakova, M. Ledvina and M. Nesladek, in *Optical Engineering of Diamond*, eds. R. Mildren and J. Rabeau, Wiley-VCH, Weinheim, 2013, pp. 209–238.
6 V. Yu. Osipov, I. D. Gridnev and A. M. Panich, *Mendeleev Commun.*, 2018, **28**, 404.
7 V. Yu. Osipov, A. E. Aleksenskiy, A. I. Shames, A. M. Panich, M. S. Shestakov and A. Ya. Vul', *Diamond Relat. Mater.*, 2011, **20**, 1234.

8 I. D. Gridnev, V. Yu. Osipov, A. E. Aleksenskii, A. Ya. Vul' and T. Enoki, *Bull. Chem. Soc. Jpn.*, 2014, **87**, 693.
9 Y. Liu, V. N. Khabashesku and N. J. Halas, *J. Am. Chem. Soc.*, 2005, **127**, 3712.
10 Y. Liu, Z. Gu, J. L. Margrave and V. N. Khabashesku, *Chem. Mater.*, 2004, **16**, 3924.
11 V. N. Khabashesku, Y. Liu and J. L. Margrave, *US Patent 7820130B2*, 2010.
12 V. N. Khabashesku, J. L. Margrave and E.V. Barrera, *Diamond Relat. Mater.*, 2005, **14**, 859.
13 T. Ando, K. Yamamoto, M. Matsuzawa, Y. Takamatsu, S. Kawasaki, F. Okino, H. Touhara, M. Kamo and Y. Sato, *Diamond Relat. Mater.*, 1996, **5**, 1021.
14 T. Ando, K. Yamamoto, M. Kamo, Y. Sato, Y. Takamatsu, S. Kawasaki, F. Okino and H. Touhara, *J. Chem. Soc., Faraday Trans.*, 1995, **91**, 3209.
15 S. Turner, O. I. Lebedev, O. Shenderova, I. I. Vlasov, J. Verbeeck and G. Van Tendeloo, *Adv. Funct. Mater.*, 2009, **19**, 2116.
16 S. Turner, O. Shenderova, F. Da Pieve, Y.-g. Lu, E. Yücelen, J. Verbeeck, D. Lamoen and G. Van Tendeloo, *Phys. Status Solidi A*, 2013, **210**, 1976.
17 V. Yu. Osipov, N. M. Romanov, F. M. Shakhov and K. Takai, *J. Opt. Technol.*, 2018, **85**, 122.
18 N. M. Romanov, V. Yu. Osipov, K. Takai, H. Touhara and Y. Hattori, *J. Opt. Technol.*, 2017, **84**, 654.
19 H. Touhara and F. Okino, *Carbon*, 2000, **38**, 241.
20 M. Dubois, K. Guérin, N. Batisse, E. Petit, A. Hamwi, N. Komatsu, H. Kharbache, P. Pirotte and M. Masin, *Solid State Nucl. Magn. Reson.*, 2011, **40**, 144.
21 K. P. Huang, P. Lin and H. C. Shih, *J. Appl. Phys.*, 2004, **96**, 354.
22 K. K. S. Lau, J. A. Caulfield and K. K. Gleason, *Chem. Mater.*, 2000, **12**, 3032.

Received: 25th June 2019; Com. 19/5966